

A model reference adaptive sliding mode control for the position control of permanent magnet synchronous motor

Proc IMechE Part I:
J Systems and Control Engineering
1–11

© IMechE 2020

Article reuse guidelines:

sagepub.com/journals-permissions

DOI: 10.1177/0959651820941954

journals.sagepub.com/home/pii



Junfeng Jiang^{1,2} , Xiaojun Zhou^{1,2}, Wei Zhao³ and Wei Li³

Abstract

A model reference adaptive sliding mode control for the position control of the permanent magnet synchronous motor is developed in this article. First of all, a fast sliding surface is designed to achieve faster convergence than the ordinary sliding mode control. Then, the adaptive laws are developed to make the control parameters, especially the switching gain, updated online. Therefore, the chattering can be reduced effectively and the disturbance can be rejected well. Finally, a reference model which produces an exponential decay curve is applied for the position error to follow. Thus, not only fast error convergence can be guaranteed, but also the dynamic process of the system response can be controlled easily by modifying the decay rate of the reference model. The proposed model reference adaptive sliding mode control scheme combines the advantages of the sliding mode control and the model reference adaptive control. Simulation and experimental results reveal that faster and more accurate performance with smoother control signal and better robustness is obtained compared with other methods. Also, the model reference adaptive sliding mode control method can maintain good performance when the system inertia or the position reference varies in a wide range.

Keywords

Permanent magnet synchronous motor, adaptive control, sliding mode control, model reference adaptive control, motion control, robust control

Date received: 20 June 2019; accepted: 12 June 2020

Introduction

The permanent magnet synchronous motor (PMSM) has been applied widely in high-performance drive systems such as robots, electric vehicles and numerical control machine tools.¹ This is a result of its high efficiency, high density compactness and high torque-to-inertia ratio. However, the performance of PMSM systems may be degraded because of external disturbances such as the load torque disturbance, the measurement error and cogging and internal uncertainties such as parameter variations. In this case, traditional linear method like proportional–integral–derivative (PID) controller cannot realize fast, accurate response and good robustness against disturbances.²

Many nonlinear methods have been proposed to enhance the performance of PMSM drives. In El-Sousy,³ an intelligent neural network control (NNC) method has been proposed to deal with the unmodeled parts of PMSM model. Besides, an adaptive NNC system has been proposed to for PMSM servo-drive electric scooter.⁴ An adaptive fuzzy controller was

developed to eliminate the interconnection effects of the PMSM in Barkat et al.⁵ In Nguyen and Jung,⁶ a model predictive control (MPC) was developed to guarantee the stability and robustness for surface-mounted PMSM drives. In addition, it has been verified that the MPC method has fast speed-tracking capacity and low switching frequency. To suppress speed ripples in PMSM systems, a plug-in iterative learning control scheme was applied in the conventional PI speed controller in Qian et al.⁷ The results demonstrate that the scheme is more effective in frequency domain. In Jin

¹State Key Laboratory of Fluid Power and Mechatronics Systems, Zhejiang University, Hangzhou, China

²Zhejiang Province Key Laboratory of Advanced Manufacturing Technology, Zhejiang University, Hangzhou, China

³Northwest Institute of Mechanical and Electrical Engineering, Xian Yang, China

Corresponding author:

Xiaojun Zhou, School of Mechanical Engineering, Zhejiang University, Hangzhou 310027, China.

Email: cmeesky@163.com

and Lee,⁸ a robust method composed of a model reference adaptive controller and a disturbance estimator has been proposed. This method compensates the cross-coupling terms regardless of parameter variations. An evolutionary fuzzy PID controller has been designed for PMSM systems in Choi et al.⁹ The fuzzy PID method shows good performance in the presence of load torque variations. The above methods have improved the control performance of PMSM systems from different perspectives. However, it should be noted that the design complexity and computational burden of these new methods are increased.¹⁰ Moreover, generalizing their designs into our application, the position control of PMSM is a question.

During the past decades, sliding mode control (SMC) has been applied widely for its fast response and robustness against disturbances.^{11,12} A non-singular terminal SMC (NTSM) has been proposed by Feng et al.¹³ and applied in the rigid manipulators. The NTSM solves the singularity problem of traditional terminal SMC (TSMC) in a simple way. A continuous NTSM (CNTSM) was proposed by Yu et al.¹⁴ to overcome the chattering problem. The simulation results show that the CNTSM has advantages of stronger robustness and chattering attenuation. However, the effectiveness of CNTSM in real PMSM systems has not been validated. The chattering problem still hinders the application of SMC.^{15,16} Numerous methods have been developed to solve the chattering problem. The boundary layer approach was introduced for the speed control of PMSM by Baik et al.¹⁷ However, the disturbance rejection capacity of SMC is weakened while the chattering phenomenon is attenuated. In addition, several disturbance estimation techniques have been studied to eliminate the chattering phenomenon by compensating for the disturbance. In Kim and Youn,¹⁸ a simple disturbance observer was presented to estimate the disturbance torque and flux linkage. An adaptive disturbance observer has been introduced for the current control of PMSM in Mohamed,¹⁹ and has achieved high current-control performance with chattering minimization. The extended state observer (ESO) has been also successfully applied for disturbance estimation and compensation.^{20–23} However, the disturbance observers make control systems complex and are usually not easily to implement in real applications. Moreover, the disturbance estimation is usually derived from the time-varying parameters such as the voltage and current of the pulse width modulation (PWM) inverter. These parameters are difficult to measure accurately because they contain much noise caused by the switching.²⁴

As a result, there are still three issues in the usage of the SMC:

1. Keeping balance between disturbance rejection capacity and control chattering cannot be realized easily. Large switching gain is usually selected to obtain strong robustness, which leads to large control input and serious chattering.^{25,26}
2. The fractional powers of the existing nonlinear sliding surface (SS) are usually between 0 and 1, which results in a slow reaching phase.
3. Although fast and accurate control performance may be achieved by adjusting SMC parameters kindly, we cannot control the dynamic process. For example, a dynamic response with a specific settling time may be necessary in the position control of PMSM drives.

An integral terminal sliding mode (ITSM) control method²⁷ has been developed for tracking control of uncertain relative-degree-one systems. Sign and fractional integral terminal sliding modes were introduced in ITSM so that the reaching time of the sliding modes is eliminated. In other words, a fast transient response is realized. However, the robustness of ITSM against external disturbances and internal uncertainties in PMSM systems cannot be guaranteed. In Wang et al.,²⁶ an ITSM control scheme with the adaptive SS has been developed for automobile electronic throttle systems. However, the conventional reaching law with a constant switching gain has been adopted so that the aforementioned issue (1) cannot be solved. In recent years, the concept of model reference adaptive sliding mode (MRASM) has been proposed for different applications. In Ganesan et al.,²⁸ a hybrid controller comprising a model reference adaptive control (MRAC) and a second-order SMC was developed for automatic train operation. A model reference adaptive SS has been proposed by Kara and Salamci²⁹ for different missile models. An MRASM method using a neural network has been reported in Fang et al.³⁰ to control the single-phase active power filter. The above methods have improved the performance of their plants. However, the effectiveness of these methods in PMSM systems remains unknown. They cannot completely solve the aforementioned three issues in PMSM control systems. In addition, the effectiveness of these MRASM methods was not verified in real applications.

In this article, a novel MRASM method is developed for the position control of PMSM. It is composed of a reference model producing exponential decay curves and a novel adaptive integral sliding mode control (AISM). The MRAC has been studied extensively for the advantages of explicit dynamic performances and parameter adaptation capabilities.^{31,32} The proposed MRASM control scheme will be on the basis of MRAC structure, and an AISM will be designed as a replacement of the conventional adaptive laws. Therefore, the proposed MRASM combines the advantages of MRAC and SMC. The contributions of this article can be listed as follows.

1. A new AISM method is designed. Control parameters including the switching gain are designed to be adaptive online. Therefore, both the disturbance rejection ability and the chattering-free characteristic can be guaranteed. Moreover, the SS has a

fractional power which is larger than 1, which can achieve faster convergence than the conventional SS. Consequently, the aforementioned issues (1) and (2) can be addressed.

2. To control the dynamic process easily, an exponential decay in Nguyen et al.¹⁰ is applied. Thus, not only the fast response but also the dynamic response with specific settling time can be realized. Therefore, the aforementioned issue (3) will be solved effectively.
3. The proposed method has been applied in the PMSM systems successfully. Simulation and experimental studies were carried out to verify the good performance of the proposed MRASM control scheme.

The rest of the article is organized as follows. Section “Mathematical model of PMSM” shows the mathematical model of PMSM under internal uncertainties and external disturbances. In section “The MRASM controller design,” the proposed MRASM control method is designed, and the closed-loop stability is proved. Simulation and experimental results are presented in section “Results and discussion.” Finally, section “Conclusion” gives the concluding remarks.

Mathematical model of PMSM

Taking the rotor coordinates d - q as reference coordinates, the mathematical model of surface-mounted PMSM can be expressed as follows³³

$$\begin{cases} u_d(t) = L_s \dot{i}_d(t) - L_s \omega_r(t) i_q(t) + R_s i_d(t) \\ u_q(t) = L_s \dot{i}_q(t) + L_s i_d(t) \omega_r(t) + \psi_r \omega_r(t) + R_s i_q(t) \\ T_e(t) = K_t i_q(t) \\ \frac{J}{n_p} \dot{\omega}_r(t) = T_e(t) - \frac{B}{n_p} \omega_r(t) - T_L \end{cases} \quad (1)$$

where $u_d(t)$, $u_q(t)$ are d and q axis stator voltages, respectively; $i_d(t)$, $i_q(t)$ are d and q axis stator currents, respectively; L_s is the normal value of stator inductance; R_s is the normal value of stator resistance; $\omega_r(t)$ is the electrical angular velocity of rotors; $T_e(t)$ is electrical magnetic torque; n_p is the number of pole pairs; K_t is the normal value of torque constant; J is the normal value of system moment of inertia; B is the normal value of viscous friction coefficient; T_L is load torque; ψ_r is the normal value of flux linkage of rotors.

Usually, to attenuate the couplings between speed and current, d -axis reference current i_d^* is set to 0.³⁴ Assume that the external disturbance and parameter variations are absent. Taking the angular position and velocity as the system state variables, the dynamic model can be expressed as

$$\begin{cases} \dot{\theta}_r(t) = \omega_r(t) \\ \dot{\omega}_r(t) = \frac{n_p K_t}{J} i_q(t) - \frac{B}{J} \omega_r(t) \\ = \frac{n_p K_t}{J} i_q^*(t) - \frac{B}{J} \omega_r(t) + \frac{n_p K_t}{J} (i_q(t) - i_q^*(t)) \\ = a i_q^*(t) + b \omega_r(t) + c(t) \end{cases} \quad (2)$$

where θ_r is the electrical angle of rotors, $a = n_p K_t / J$, $b = -B/J$, $c(t) = a(i_q(t) - i_q^*(t))$.

If the disturbances occur, that is, a load torque disturbance or parameter variations effect the system, the dynamic model of PMSM drives can be modified as

$$\begin{cases} \dot{\theta}_r(t) = \omega_r(t) \\ \dot{\omega}_r(t) = (a + \Delta a) i_q^*(t) + (b + \Delta b) \omega_r(t) + c(t) - T_L \\ = a i_q^*(t) + b \omega_r(t) + d(t) \end{cases} \quad (3)$$

where $d(t)$ is called lumped disturbance and defined as

$$d(t) = \Delta a i_q^*(t) + \Delta b \omega_r(t) + c(t) - T_L \quad (4)$$

Here, the bound of the lumped disturbance is given as follows

$$|d(t)| < \eta_0 \quad (5)$$

where η_0 is a given positive constant.

Remark 1: In real industrial applications, the load torque and the system inertia variation are two main disturbances. Although it is hard to obtain their maximum in a PMSM drives without operating conditions, it is not difficult to know their bound in a specific application. That is, the bound η_0 can be obtained according to Equation (4) in a given application.

The MRASM controller design

The field oriented vector control for PMSM position control systems has been used widely. It has a cascade structure including a position loop, a speed loop and two current loops. In this article, the position loop and the speed loop are to be unified (herein after called position-speed loop).

This section presents a new adaptive sliding mode control based on a reference model. First, a reference model introduced by Nguyen et al.¹⁰ is adopted. It produces an exponential decay curve for the position error to follow. Next, an AISMC with a fast integral SS and an adaptive switching gain is designed. Thus, a MRASM controller is developed for the position control of PMSM systems. Finally, the stability of the overall system is proved using Lyapunov method.

Reference model selection

The selected reference model can be expressed as¹⁰

$$\dot{e}_m + \lambda_m e_m = 0 \quad (6)$$

with e_m is the output of reference model and λ_m is a positive constant parameter. Unlike the traditional MRAC whose reference model offers reference for the feedback position, this reference model output is compared with the position error ($e = \theta_r - \theta_{ref}$ with θ_{ref} the position reference) directly. The reference model output can be represented as the following experimental decay form

$$e_m = c(e^{-\lambda_m})^t \quad (7)$$

where $c > 0$ is deduced from the initial condition and t is the time. One can see that the decay rate can be controlled by modifying λ_m . Assume that the position error e tracks e_m well. The position error can converge to 0 in finite time and the convergence time can be regulated easily. Define the system state variable $x_1 = e - e_m$, the error dynamic model can be represented as

$$\begin{cases} \dot{x}_1 = x_2 \\ \dot{x}_2 = \ddot{\theta}_r(t) - \ddot{\theta}_{ref}(t) - \ddot{e}_m = at_q^*(t) + b\omega_r(t) \\ \quad + d(t) - \ddot{\theta}_{ref}(t) - \ddot{e}_m \end{cases} \quad (8)$$

MRASM controller design

We design the following novel adaptive integral SS for dynamic model (8)

$$s = \dot{x}_1 + \beta(t)x_1^\gamma + \alpha x_I \quad (9)$$

$$\dot{x}_I(t) = x_1^{q/p}(t) \quad (10)$$

with $\gamma > 1$ is a designed parameter, $\beta(t)$ can be updated online by the following adaptive laws, α is a positive parameter, p and q are odd integers satisfying $p > q > 0$. The initial condition is $x_I(0) = -1/\alpha [\dot{x}_1(0) + \beta(0)x_1^\gamma(0)]$ with $\beta(0)$ the initial value of $\beta(t)$. The proposed MRASM control scheme is designed as follows

$$\begin{aligned} t_q^* &= \frac{1}{a} \\ (\ddot{\theta}_{ref} + \ddot{e}_m - b\omega_r - \beta(t)\gamma x_1^{\gamma-1}\dot{x}_1 - \alpha x_1^{q/p} - \eta(t)\text{sign}(s) - ks) \end{aligned} \quad (11)$$

where $\eta(t)$ is another parameter that can be updated online, k is designed to be positive. $\beta(t)$ and $\eta(t)$ are adjusted by the adaptive laws as

$$\dot{\beta}(t) = -k_1 x_1^{2-\gamma} s \quad (12)$$

$$\dot{\eta}(t) = k_2 |s| \quad (13)$$

where k_1 and k_2 are two positive parameters which determine the adaptive rates of the control parameters.

Remark 2: The proposed method is different from the previous reported AISMC in Wang et al.²⁶ First of all, the switching gain in this article is designed to be adaptive online. This is important for the chattering reduction and the robustness improvement. Second, the adaptive law of $\beta(t)$ is modified to be more effective especially when the x_1 close to 0. Finally, as mentioned before, the SS is designed to assure faster convergence.

Remark 3: The SS of conventional ITSM control in Chiu²⁷ can be expressed as

$$s_I = \dot{x}_1 + \beta_0 x_1 + \alpha_0 x_I \quad (14)$$

$$\dot{x}_I(t) = x_1^{q/p}(t) \quad (15)$$

where β_0 and α_0 are two positive parameters; and p and q are the same as those in Equation (10). When the system states reach the SS (i.e. $s = s_I = 0$), the following equation can be deduced according to equations (9) and (14), respectively

$$\dot{x}_1 = -\beta_0 x_1 - \alpha_0 x_I \quad (16)$$

$$\dot{x}_1 = -\beta(t)x_1^\gamma - \alpha x_I \quad (17)$$

Assume that $\beta_0 = \beta(t)$ and $\alpha_0 = \alpha$. One can see that the absolute value of \dot{x}_1 in Equation (16) is smaller compared with that of Equation (17) when x_1 is far away from zero. In other words, the convergence rate of conventional method is slower than that of the proposed method. This will also be validated by the following simulations and experiments.

Remark 4: Non-singularity and fast response are two main advantages of ITSM control. We can enable the system states to start on the SS $s = 0$ by adjusting the initial value of x_I . Therefore, reaching phase can be eliminated and fast response can be obtained. In addition, one can see from control law (11) that there is no negative fractional power in the control law. In other words, the proposed control scheme is non-singular.

Theorem: Consider the PMSM systems with the error dynamic model in dynamic model (8), the error x_1 and its first derivative x_2 will have a finite-time convergence to 0 if the control law is designed as Equation (11) with the adaptive laws in Equations (12) and (13).

Proof: The disturbance bound error is defined as $\tilde{\eta} = \eta(t) - \eta_0$. Choosing a Lyapunov function as

$$V = \frac{1}{2}s^2 + \frac{1}{2k_2}\tilde{\eta}^2 \quad (18)$$

Then, the derivative of the Lyapunov function is

$$\begin{aligned} \dot{V} &= s\dot{s} + \frac{1}{k_2}(\eta(t) - \eta_0)\dot{\eta}(t) \\ &= s(\dot{x}_2 + \dot{\beta}(t)x_1^\gamma + \gamma\beta(t)x_1^{\gamma-1}\dot{x}_1 + \alpha x_1^{q/p}) \\ &\quad + \frac{1}{k_2}(\eta(t) - \eta_0)\dot{\eta}(t) \\ &= s(at_q^*(t) + b\omega_r(t) + d(t) - \ddot{\theta}_{ref} - \ddot{e}_m + \dot{\beta}(t)x_1^\gamma \\ &\quad + \gamma\beta(t)x_1^{\gamma-1}\dot{x}_1 + \alpha x_1^{q/p}) + \\ &\quad \frac{1}{k_2}(\eta(t) - \eta_0)\dot{\eta}(t) \end{aligned} \quad (19)$$

Substituting the control law (11) into Equation (19) yields

$$\begin{aligned}
\dot{V} &= s \left[(\ddot{\theta}_{ref} + \ddot{e}_m - b\omega_r - \beta(t)\gamma x_1^{\gamma-1} x_2 - \alpha x_1^{q/p} - \eta(t)\text{sign}(s) - ks) + b\omega_r(t) \right. \\
&\quad \left. + d(t) - \ddot{\theta}_{ref} - \ddot{e}_m + \dot{\beta}(t)x_1^\gamma + \gamma\beta(t)x_1^{\gamma-1} x_2 + \alpha x_1^{q/p} \right] + \frac{1}{k_2} (\eta(t) - \eta_0) \dot{\eta}(t) \\
&= s \left[d(t) + \dot{\beta}(t)x_1^\gamma - \eta(t)\text{sign}(s) - ks \right] + \frac{1}{k_2} (\eta(t) - \eta_0) \dot{\eta}(t) \\
&= sd(t) + s\dot{\beta}(t)x_1^\gamma - |s|\eta(t) - ks^2 + \frac{1}{k_2} (\eta(t) - \eta_0) \dot{\eta}(t)
\end{aligned} \tag{20}$$

Using the updated laws (12) and (13), we have

$$\begin{aligned}
\dot{V} &= sd(t) - k_1 s^2 x_1^2 - |s|\eta(t) - ks^2 + (\eta(t) - \eta_0)|s| \\
&= -k_1 s^2 x_1^2 - ks^2 - \eta_0 |s| + sd(t) \\
&\leq -k_1 s^2 x_1^2 - ks^2 - \eta_0 |s| + |s||d(t)| \\
&= -k_1 s^2 x_1^2 - ks^2 - (\eta_0 - |d(t)|)|s|
\end{aligned} \tag{21}$$

Equations (5) and (21) imply that $\dot{V} < 0$, which shows that x_1 and x_2 converge to 0. This completes the proof.

The above proof reveals that the position error e converges to the reference model output e_m in finite time. It is obvious that e_m converges to 0 in an exponential decay way, therefore, e converges to 0 in finite time. Figure 1 shows the complete block diagram of the proposed MRASM for the position control of PMSM systems.

Results and discussion

To verify the performance of the proposed method, simulations and experiments were carried out in MATLAB/Simulink R2017a and a digital signal processing (DSP)-based test environment, respectively. The position control can be divided into positioning control and tracking control, and they will be illustrated in simulations and experiments, respectively. In our test bench, the load disturbance and the inertia variation are the major parts of external disturbances and

internal uncertainties, respectively. As a result, only the load disturbance and the inertia variation are considered in this article for simplicity. For comparison, the ITSM control²⁷ and the method in Ganesan et al.²⁸ (hereafter called as model reference adaptive second-order sliding mode (MRASOSM)) were modified for the position control of PMSM systems. They are presented as follows

$$\begin{aligned}
u_{\text{ITSM}} &= \frac{1}{a} \\
(\ddot{\theta}_{ref} - b\omega_r - \beta_0 \dot{e} - \alpha_0 e^{q/p} - k_3 \text{sign}(s_1) - k_4 s_1)
\end{aligned} \tag{22}$$

where α_0 , β_0 , p , q and s_1 are the same as those in Equations (14) and (15), k_3 and k_4 are two positive parameters

$$u_{\text{MRASOSM}} = \hat{k}_{s1} |s_m|^{0.5} \text{sign}(s_m) + \int \hat{k}_{s2} \text{sign}(s_m) dt \tag{23}$$

with

$$\begin{aligned}
s_m &= \theta_{ref} - \theta_r \\
\dot{x}_m &= a_m x_m + b_m \theta_{ref} \\
e_m &= \theta_r - x_m \\
\dot{\hat{k}}_{s1} &= - \left(\Gamma_{s1} |s_m|^{0.5} \text{sign}(s_m) e_m + \gamma_{s1} \hat{k}_{s1} \right) \\
\dot{\hat{k}}_{s2} &= - \left(\Gamma_{s2} \left(\int \text{sign}(s_m) dt \right) e_m + \gamma_{s2} \hat{k}_{s2} \right)
\end{aligned}$$

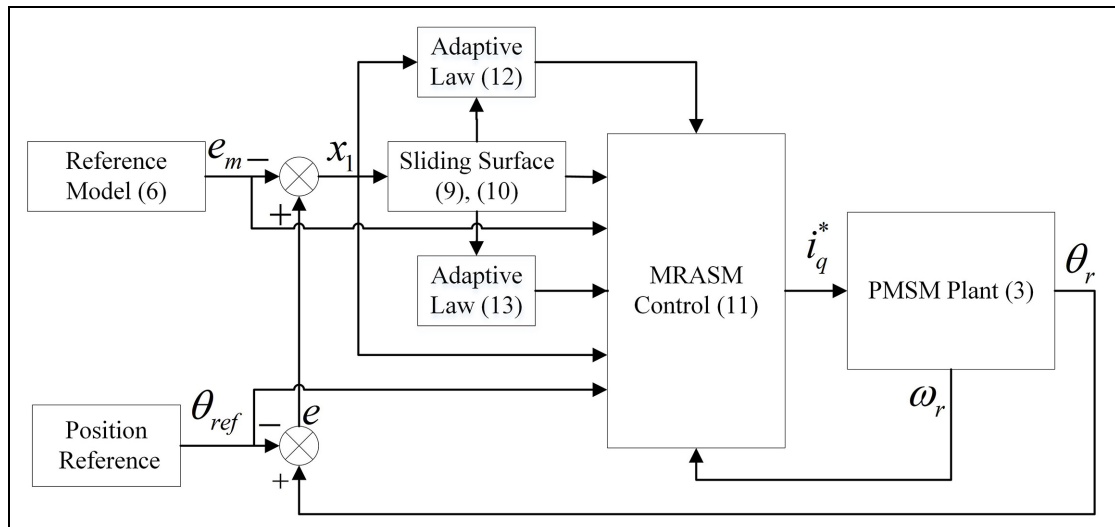


Figure 1. The block diagram of the proposed MRASM control scheme.

Table 1. Parameters of the PMSM.

Parameters	Values
Rated power	1.5 KW
Rated torque	14.32 Nm
Rated speed	1000 rpm
Stator resistance	1.79 Ω
Pole pairs	4
Torque constant	2.45 Nm/A
System moment of inertia	1.792×10^{-3} kg m ²
Viscous friction coefficient	9.403×10^{-5} Nm s/rad
Stator inductance	6.68×10^{-3} H
Flux linkage	0.4083 Wb

where \hat{k}_{s1} and \hat{k}_{s2} are the adaptive control gains, s_m is the sliding mode surface of MRASOSM, a_m and b_m are the parameters of reference model, x_m is the output of the reference model and e_m is used to update the adaptive control gains.

The saturation limit of control input i_q^* is ± 25 A and the disturbance bound $\eta_0 = 10$. The sample time of position-speed loop and current loop are 10 and 1 ms, respectively. Note that every control algorithm obtains relatively good performance by adjusting its parameters. Parameters of the PMSM are shown in Table 1.

Simulation results

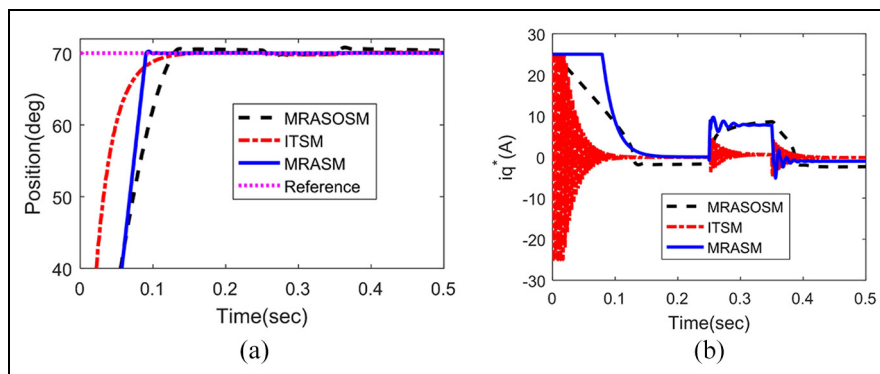
This part validates the positioning performance of the proposed method. The PMSM positioning systems under MRASOSM scheme, ITSM control and the proposed MRASM control method were simulated by MATLAB/Simulink R2017a. The proportional and integral gain of current loop are 0.15. The MRASOSM parameters are $\Gamma_{s1} = \Gamma_{s2} = 0.001$, $\gamma_{s1} = \gamma_{s2} = 0.5$, $a_m = -10$, $b_m = 10$ and $\hat{k}_{s1}(0) = \hat{k}_{s2}(0) = 2$. Parameters of ITSM were selected as: $\alpha_0 = 100$, $\beta_0 = 250$, $p = 7$, $q = 1$, $k_3 = 250$, $k_4 = 50$. The following parameters of MRASM were used: $\lambda_m = 50$, $\alpha = 50$, $\beta(0) = 150$, $\gamma = 1.9$, $\eta(0) = 50$, $k_1 = 0.002$, $k_2 = 0.01$, p and q are the same as those in ITSM control.

Positioning responses with load disturbance. For comparison, the position reference is $\theta^* = 70^\circ$, which can lead to relatively good performance for MRASOSM controller and ITSM control. To demonstrate the disturbance rejection ability of the proposed method, external load torque $T_L = 5$ Nm is added at $t = 0.25$ s and removed at $t = 0.35$ s.

The simulation results of three methods are shown in Figure 2. One can see that MRASOSM shows smooth control signal, but large fluctuations are caused by the external load disturbance. Moreover, the steady-state error is large. ITSM shows finite-time convergence and small fluctuation caused by load disturbance. However, the convergence rate is a little slow and we can observe a large control chattering from Figure 2(b). The result reveals that we can obtain a good disturbance rejection ability by choosing a large switching gain k_4 . On the contrary, however, the chattering level is increased because of the large gain. It is difficult to keep a good balance between chattering and robustness using ITSM control. It can be observed that fast, accurate performance is obtained when MRASM is applied, and the disturbance fluctuation is negligible. Moreover, Figure 2(b) shows that the control signal is smooth even though the load disturbance varies.

Positioning responses with inertia variation. To demonstrate the uncertainty rejection ability of the proposed method, the system inertia is increased to $10J_0$ and the performances of three methods are shown in Figure 3. It is obvious that the proposed MRASM method has faster and more accurate performance compared with MRASOSM and ITSM control. Furthermore, the control signal of MRASM control is smooth.

Positioning adjustability of MRASM. Position targets with large range are applied for PMSM systems under MRASM control. Figure 4(a) and (b) shows the simulation results for target position 150° and 250° , respectively. One can see that a finite-time convergence can be guaranteed even if the position demand becomes large.

**Figure 2.** Positioning performance of three controllers with load disturbance (simulation): (a) position response and (b) control input i_q^* .

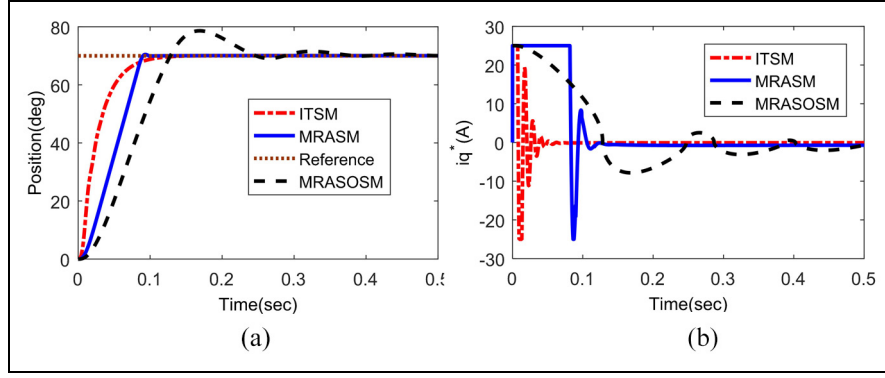


Figure 3. Positioning performance of three controllers with $J = 10J_0$ (simulation): (a) position response and (b) control input i_q^* .

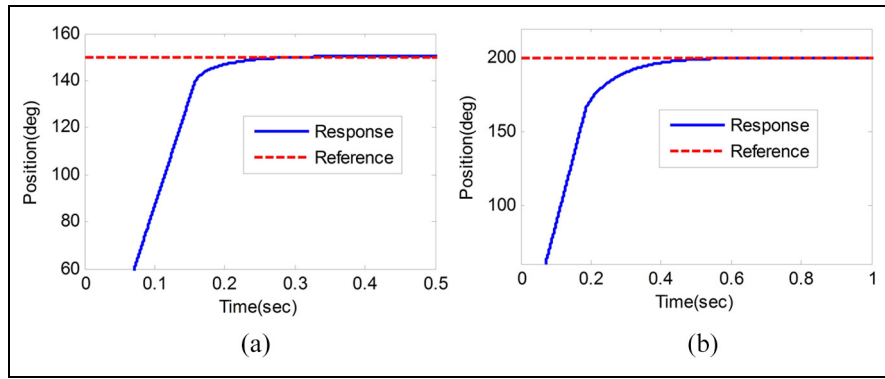


Figure 4. Positioning performance of MRASM controller under different position references (simulation): (a) reference = 150° and (b) reference = 200° .

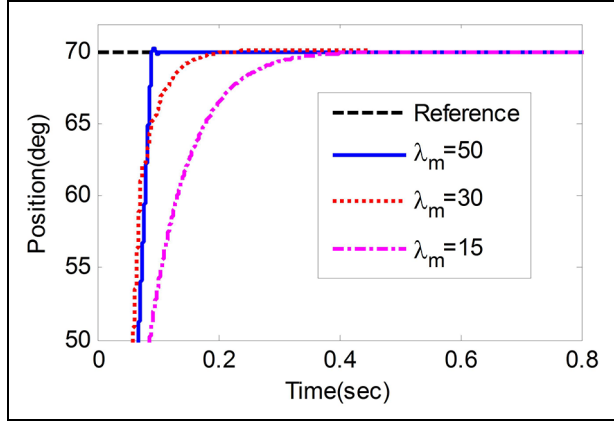


Figure 5. Positioning performance of MRASM controller under different values of λ_m (simulation).

Figure 5 presents the performance of the MRASM control with different values of λ_m in the reference model. It is obvious that we can regulate the transient process easily by adjusting λ_m .

Experimental results

This part demonstrates the tracking performance of the proposed MRASM control. An experimental setup has

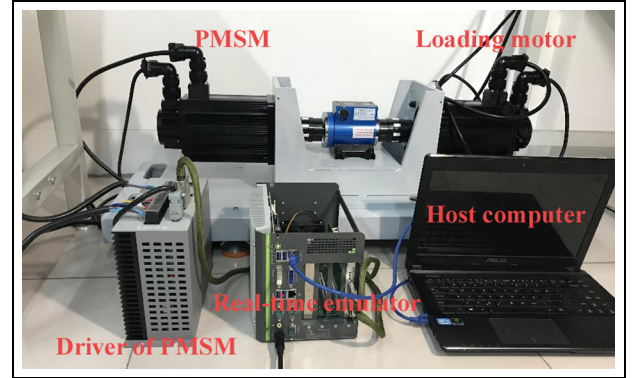


Figure 6. Experimental test setup.

been built as shown in Figure 6. The real-time emulator contains a DSP TMS320F28335PGFA. The function of it is to provide a MATLAB/Simulink programming environment. The whole algorithm, including position-speed controller, Clarke transform, inverse Park transform and so on, is implemented by MATLAB/Simulink. Then, all of those algorithms are converted into DSP code. Next, the gate drive is sent from DSP to the driver of PMSM. The experimental data can be collected on the host computer. An incremental position encoder is used to measure the rotor speed and

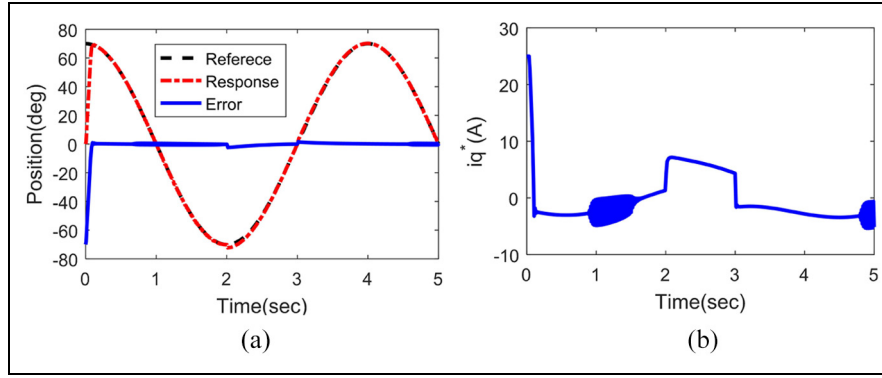


Figure 7. Tracking performance of MRASOSM with load disturbance (experiment): (a) position response and (b) control input i_q^* .

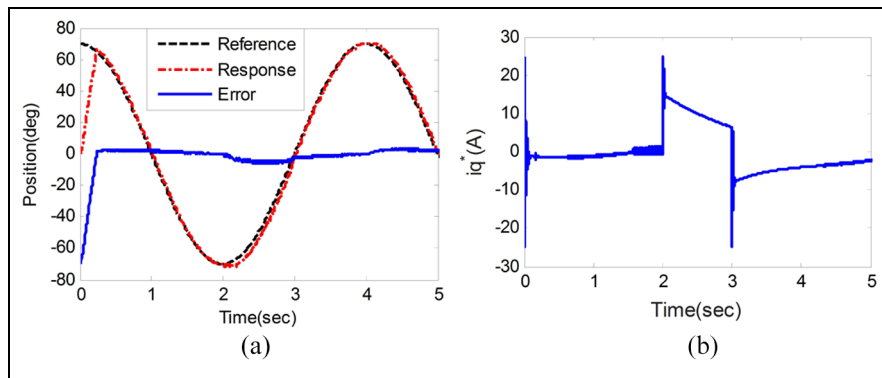


Figure 8. Tracking performance of ITSM with load disturbance (experiment): (a) position response and (b) control input i_q^* .

absolute rotor position. Hall-effect devices are used to measure the phase currents.

The MRASOSM parameters are $\Gamma_{s1} = \Gamma_{s2} = 0.001$, $\gamma_{s1} = \gamma_{s2} = 0.5$, $a_m = -10$, $b_m = 10$ and $\hat{k}_{s1}(0) = \hat{k}_{s2}(0) = 5$. The parameters of ITSM were selected as: $\alpha_0 = 100$, $\beta_0 = 250$, $p = 7$, $q = 3$, $k_3 = 200$ and $k_4 = 50$. The following parameters of MRASM were used: $\lambda_m = 20$, $\alpha = 50$, $\beta(0) = 50$, $\gamma = 1.9$, $\eta(0) = 50$, $k_1 = 0.002$ and $k_2 = 0.01$. p and q are the same as those in ITSM control.

Tracking performances with load disturbance. For comparison, the position reference is $\theta^* = 70 \sin((\pi/2)t + (\pi/2))^\circ$, which can lead to relatively good performance for MRASOSM controller and ITSM control. External load torque $T_L = 5 \text{ Nm}$ is added at $t = 2 \text{ s}$ and removed at $t = 3 \text{ s}$.

We can see from Figure 7 that MRASOSM shows fast convergence. However, the disturbance rejection ability is poor. Figure 8 shows the performance of ITSM. It can be observed that the tracking error converges to a small region in finite time. However, a large amount of chattering is caused in the control signal. Moreover, there is an evident fluctuation in the position response and the control input when the load torque varies. The performance of the proposed method are given in Figure 9. A faster response is realized than

the ITSM control due to the application of the proposed fast SS. The control input is smooth regardless the disturbance, and the response fluctuation is negligible when the load disturbance occurs. It should be emphasized that due to the adaptation mechanism, the chattering can be reduced and the load disturbance can be rejected.

Tracking performance with inertia variation. To validate the uncertainty rejection capability of MRASM control scheme further, we change the system inertia of the experimental test setup. The reference is still $\theta^* = 70 \sin((\pi/2)t + (\pi/2))^\circ$ and the tracking error of the MRASM method is shown in Figure 10. It can be seen that the convergence rate becomes a little slower with an increase in the system inertia. However, the transient response remains fast and accurate regardless of the internal parameter variations. Thus, we can conclude that the proposed method has strong robustness against external disturbances and internal parameter variations.

Tracking adjustability of MRASM. Tracking targets with large range are applied for PMSM systems under MRASM control. Figure 11(a)–(c) shows the experimental results for target position $100 \sin(\pi t + \pi/2)^\circ$

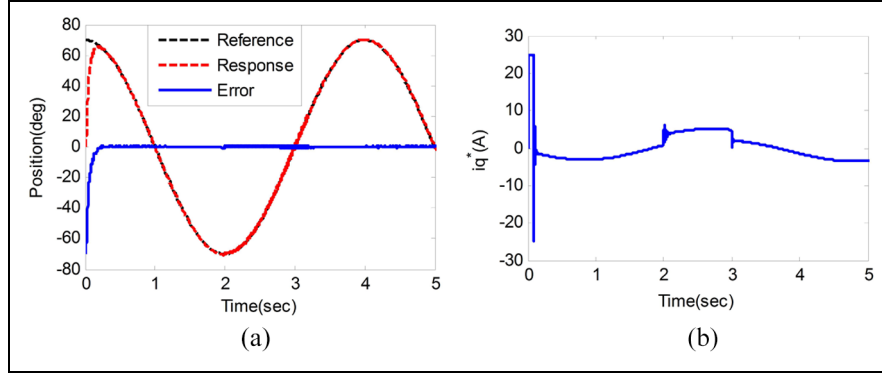


Figure 9. Tracking performance of MRASM with load disturbance (experiment): (a) position response and (b) control input i_q^* .

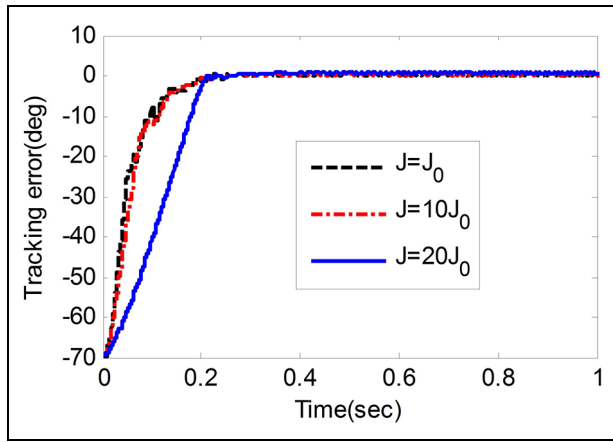


Figure 10. Tracking error of MRASM control with different system inertias (experiment).

and $160\sin(\pi t + \pi/2)^\circ$, respectively. It can be observed that fast, accurate performance can be obtained even if the amplitude and frequency of tracking target become large.

Figure 12 provides the tracking performance of MRASM control with different values of λ_m in the reference model. One can see that the transient process can be controlled easily by adjusting λ_m . Note that this

is difficult for conventional SMC methods. It is the use of reference model that achieves the adjustability of transient response.

Discussion

To make comparisons clear, the positioning performances with load disturbance mentioned in section “Positioning responses with load disturbance” and the tracking performances in section “Tracking performance with inertia variation” of three methods are summarized in Table 2. For positioning task, it can be observed that the settling time of MRASM is reduced by 30.8% and 43.7% compared with MRASOSM controller and ITSM method, respectively. The steady tracking error is reduced by 83.8% and 37.5%. For tracking task, the steady tracking error is reduced by 10.9% and 85.4%. The convergence rate of MRASM is increased by 30.8% compared with ITSM method. MRASOSM shows good tracking performance but poor disturbance rejection ability. The robustness against external disturbances and internal uncertainties of the proposed method is much better than the other two controllers. It should be noted that the chattering problem is solved effectively by applying adaptive gains.

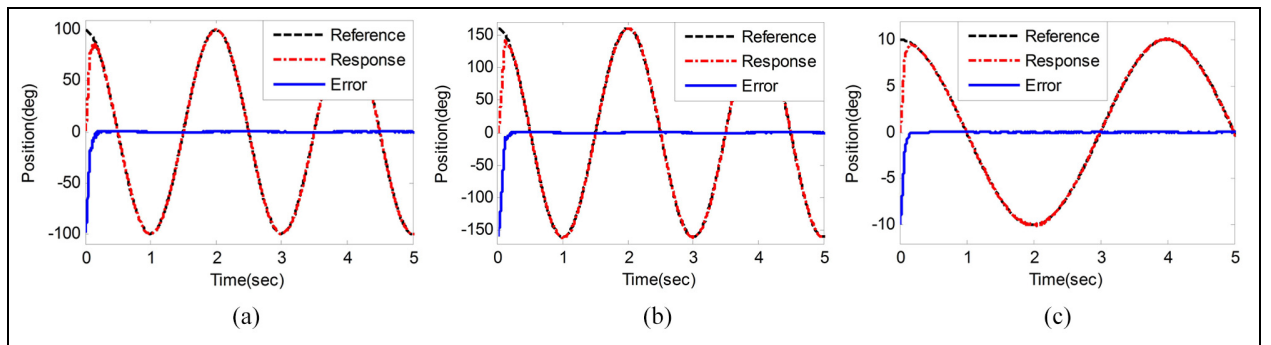


Figure 11. Tracking performance of MRASM under different references (experiment): (a) reference = $100\sin(\pi t + \pi/2)$, (b) reference = $160\sin(\pi t + \pi/2)$, and (c) reference = $10\sin(\pi/2 t + \pi/2)$ deg.

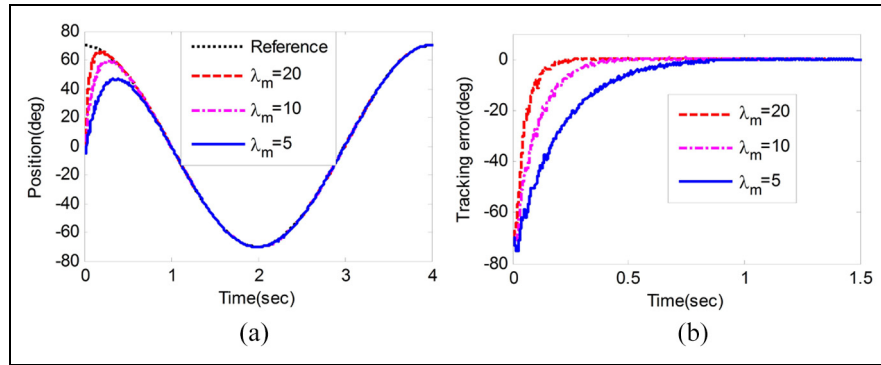


Figure 12. Tracking performance of MRASM under different values of λ_m (experiment): (a) position response and (b) tracking error.

Table 2. Control performance comparisons.

Control task	Controller	Settling time (s)	Steady-state error (°)	Maximum disturbance fluctuation (°)
Positioning task	MRASOSM	0.13	0.31	0.61
	ITSM	0.16	0.08	0.26
	MRASM	0.09	0.05	0.10
Tracking task	MRASOSM	0.12	0.46	2.01
	ITSM	0.26	2.80	2.17
	MRASM	0.18	0.41	0.98

MRASOSM: model reference adaptive second-order sliding mode; ITSM: integral terminal sliding mode; MRASM: model reference adaptive sliding mode.

Conclusion

A MRASM control scheme has been developed for the position control of PMSM systems in this article. First, a new AISMC with a fast SS and two adaptive gains is designed. The convergence rate is faster than the conventional SMC methods, and the two main control gains can be updated online to reduce chattering and reject disturbances. Second, a reference model is applied to achieve explicit dynamic performance. It produces an exponential decay curve for the position error to follow. The effectiveness of the proposed MRASM control has been illustrated by simulation and experimental results. The MRASM control shows a fast transient response, a accurate steady state, smooth control signals and good robustness against disturbance and uncertainties. In addition, the proposed method can maintain good performance when the position reference varies in a wide range. Note that the dynamic response can be regulated easily by using the proposed MRASM method. The new control scheme can be applied to other relevant servo systems.


Declaration of conflicting interests

The author(s) declared no potential conflicts of interest with respect to the research, authorship, and/or publication of this article.

Funding

The author(s) received no financial support for the research, authorship, and/or publication of this article.

ORCID iD

Junfeng Jiang  <https://orcid.org/0000-0001-5201-8753>

References

- Shyu KK, Lai CK, Tsai YW, et al. A newly robust controller design for the position control of permanent-magnet synchronous motor. *IEEE Trans Ind Electr* 2002; 49: 558–565.
- Dinh TX and Ahn KK. Adaptive-gain fast nonsingular terminal sliding mode for position control of a piezo positioning stage. *Proc IMechE, Part I: J Systems Control Engineering* 2018; 232: 994–1014.
- El-Sousy FFM. Hybrid H-infinity-based wavelet-neural-network tracking control for permanent-magnet synchronous motor servo drives. *IEEE Trans Ind Electr* 2010; 57: 3157–3166.
- Lin C-H. Adaptive recurrent Chebyshev neural network control for permanent magnet synchronous motor servo-drive electric scooter. *Proc IMechE, Part I: J Systems Control Engineering* 2014; 228: 699–714.
- Barkat S, Tlemcani A and Nouri H. Noninteracting adaptive control of PMSM using interval type-2 fuzzy logic systems. *IEEE Trans Fuzzy Syst* 2011; 19: 925–936.
- Nguyen HT and Jung J-W. Finite control set model predictive control to guarantee stability and robustness for surface-mounted PM synchronous motors. *IEEE Trans Ind Electr* 2018; 65: 8510–8519.
- Qian W, Panda SK and Xu JX. Speed ripple minimization in pm synchronous motor using iterative learning control. *IEEE Trans Energy Convers* 2005; 20: 53–61.
- Jin H and Lee J. An RMRAC current regulator for permanent-magnet synchronous motor based on statistical model interpretation. *IEEE Trans Ind Electr* 2009; 56: 169–177.
- Choi HH, Yun HM and Kim Y. Implementation of evolutionary fuzzy pid speed controller for pm synchronous motor. *IEEE Trans Ind Inform* 2015; 11: 540–547.
- Nguyen AT, Rafiq MS, Choi HH, et al. A model reference adaptive control based speed controller for a surface-mounted permanent magnet synchronous motor drive. *IEEE Trans Ind Electr* 2018; 65: 9399–9409.

11. Zhang XZ and Wang YN. Fuzzy variable structure control based on a Takagi-Sugeno model for permanent-magnet synchronous motors. *Proc IMechE, Part I: J Systems Control Engineering* 2009; 223: 773–783.
12. Taleb M and Plestan F. Adaptive robust controller based on integral sliding mode concept. *Int J Contr* 2016; 89: 1788–1797.
13. Feng Y, Yu X and Man Z. Non-singular terminal sliding mode control of rigid manipulators. *Automatica* 2002; 38: 2159–2167.
14. Yu S, Yu X, Shirinzadeh B, et al. Continuous finite-time control for robotic manipulators with terminal sliding mode. *Automatica* 2005; 41: 1957–1964.
15. Feng Y, Han F and Yu X. Chattering free full-order sliding-mode control. *Automatica* 2014; 50: 1310–1314.
16. Al-Ghanimi A, Zheng J and Man Z. A fast non-singular terminal sliding mode control based on perturbation estimation for piezoelectric actuators systems. *Int J Contr* 2016; 90: 480–491.
17. Baik IC, Kim KH and Youn MJ. Robust nonlinear speed control of PM synchronous motor using boundary layer integral sliding mode control technique. *IEEE Trans Contr Syst T* 2000; 8: 47–54.
18. Kim KH and Youn MJ. A nonlinear speed control for a PM synchronous motor using a simple disturbance estimation technique. *IEEE Trans Ind Electr* 2002; 49: 524–535. Article.
19. Mohamed Y. Design and implementation of a robust current-control scheme for a PMSM vector drive with a simple adaptive disturbance observer. *IEEE Trans Ind Electr* 2007; 54: 1981–1988.
20. Yuan Y, Yu Y, Wang ZD, et al. A sampled-data approach to nonlinear ESO-based active disturbance rejection control for pneumatic muscle actuator systems with actuator saturations. *IEEE Trans Ind Electr* 2019; 66: 4608–4617.
21. Zhao ZL and Guo BZ. A novel sxtended state observer for output tracking of MIMO systems with mismatched uncertainty. *ITAC* 2018; 63: 211–218.
22. Sayem AHM, Cao ZW and Man ZH. Model free ESO-based repetitive control for rejecting periodic and aperiodic disturbances. *IEEE Trans Ind Electr* 2017; 64: 3433–3441.
23. Huang Y and Cheng G. A robust composite nonlinear control scheme for servomotor speed regulation. *Int J Contr* 2014; 88: 104–112.
24. Kim KH. Model reference adaptive control-based adaptive current control scheme of a PM synchronous motor with an improved servo performance. *IET Electr Power App* 2009; 3: 8–18.
25. Moreno JA, Negrete DY, Torres-González V, et al. Adaptive continuous twisting algorithm. *Int J Contr* 2015; 89: 1798–1806.
26. Wang H, Li Z, Jin X, et al. Adaptive integral terminal sliding mode control for automaticaobile electronic throttle via an uncertainty observer and experimental validation. *IEEE Trans Veh Technol* 2018; 67: 8129–8143.
27. Chiu C-S. Derivative and integral terminal sliding mode control for a class of MIMO nonlinear systems. *Automatica* 2012; 48: 316–326.
28. Ganesan M, Ezhilarasi D and Jijo B. Hybrid model reference adaptive second order sliding mode controller for automatic train operation. *IET Control Theory App* 2017; 11: 1222–1233.
29. Kara F and Salamci MU. Model reference adaptive sliding surface design for nonlinear systems. *IEEE Trans Ind Appl* 2018; 54: 611–624.
30. Fang YM, Fei JT and Ma KQ. Model reference adaptive sliding mode control using rbf neural network for active power filter. *Int J Electr Power Energy Syst* 2015; 73: 249–258.
31. Zu H, Zhang GB, Fei SM, et al. Robust control for a direct-driven permanent magnetic synchronous generator without mechanical sensors based on model reference adaptive backstepping control method. *Proc IMechE, Part I: J Systems Control Engineering* 2012; 226: 1130–1141.
32. Guo L and Parsa L. Model reference adaptive control of five-phase IPM motors based on neural network. *IEEE Trans Ind Electr* 2012; 59: 1500–1508.
33. Li S and Liu Z. Adaptive speed control for permanent-magnet synchronous motor system with variations of load inertia. *IEEE Trans Ind Electr* 2009; 56: 3050–3059.
34. Wang H, Li S, Lan Q, et al. Continuous terminal sliding mode control with extended state observer for PMSM speed regulation system. *T I Meas Control* 2017; 39: 1195–1204.